Study on the coastal bathymetry based on Sentinel-2 satellite image and GEBCO data

GyongBong Ju[1], CholMin Won[1], UnChol RI[1], CholJu Kim[2]

[1] Ham hung University of Hydraulics and Power, Ham Hung, DPR of Korea

[2] **KIM IL SUNG** University, Pyongyang, D P R of Korea

Abstract

This article proposes a new bathymetry in coastal areas based on multi-spectral satellite images (Sentinel-2 satellite images) and GEBCO (General Bathymetric Chart of the Oceans) data. To measure the water depth of the coastal area, an empirical model has selected, and a new model has obtained by interpreting the relationship between each element of the model and the spectral band of the Sentinel-2 satellite image. Also, a sunlight reflection correction model has established to overcome the effect of sunlight reflection, one of the main factors that limit the accuracy of remotely sensed data. Linear regression analysis is performed between the results derived from the new model and the GEBCO data to determine the coefficients and then used the raster calculator to get the desired results. Field bathymetry data is expensive and difficult to obtain, but Sentinel-2 satellite images and GEBCO data can be downloaded for free from the website at any time. Therefore, it is easy to measure a wide range of coastal water depths in a short time using this method. The proposed bathymetry can quickly realize using QGIS spatial analysis tools.

Keyword: Satellite Images, coastal bathymetry, Linear Regression Analysis, Raster

1. Introduction

Bathymetry plays a very significant role in predicting marine risks and evaluating environmental hazards. It is also an essential environmental parameter for studying and modeling hydrodynamics, sediment transport, and coastal morphological evolution. Therefore, accurate bathymetry data is a primary task in solving many marine problems [1-7]. Field bathymetry is not only expensive for operation but also takes a long time. Due to the limitations of the regional environment, the bathymetry data of some regions is insufficient [8]. Also, bathymetry on ships has greatly influenced by weather conditions. With the advancement of aerial photography technology, radar, and remote sensing technology, bathymetry by satellite has recognized as an excellent method to measure a wide range of space at a cheaper cost than conventional acoustic measurement [9-11]. However, the accuracy of depth information decreases due to the influence of green plants, suspended sediments, and the atmosphere, so the demand for spectrum analysis in remote sensing is very high [12]. The previous study provides a method for estimating the depth in shallow parts of the sea by analyzing the coastal gravitational waves observed in a high-resolution satellite image [13]. The bathymetry inversion system cBathy has based on the dispersion relationship and the linear wave hypothesis under shallow conditions. It has combined an imaging technique with remote sensing, UAV (Unmanned Aerial Vehicle) systems, or GIS (Geographic Information System) to obtain the parameters needed for bathymetry inversion [14-19]. In the beginning stages, aerial photography, radar, or remote sensing technology has used to get the spatial-time sequence digital image or video image of surface waves in the target area [14, 18]. The acquired sea surface image or video image is identified and analyzed to obtain wave distribution information, and replaced with a dispersion relation model for calculating the depth. This bathymetry not only overcomes the low accuracy due to the water environment but also can obtain a wide range of water depths in real-time at a low cost. Therefore, this method has an advantage over the existing measurement technology. However, the accuracy of depth inversion directly depends on knowledge of good functional dispersion relationships [20]. Multispectral satellite images provide the supplementary data that are useful in solving operational and research problems. The current development of the multi-source bathymetry reconstruction promotes the public use of observations for various sources and qualities. This paper, which describes a simple and robust method for the inversion of bathymetry, is written from this

perspective. The fundamental purpose of this paper is to propose a method for measuring the water depth in the coastal area using Sentinel-2 satellite images and GEBCO depth measurement data, which can be easily has obtained. This paper has established as follows.

-Sentinel2 image selection and preprocessing for the research area
-Calibration of bathymetry model
-Bathymetry calculation using QGIS
-Result analysis

2. Study Area and Datasets

2.1 Study Area

The research area is the Wonsan Kalma Coast of the Democratic People's Republic of Korea, which is building as a world-class tourist area. The domain extends to 39 ° 14'N-39 ° 19'N and 127 ° 48'E-127 ° 52'E (Fig.1).
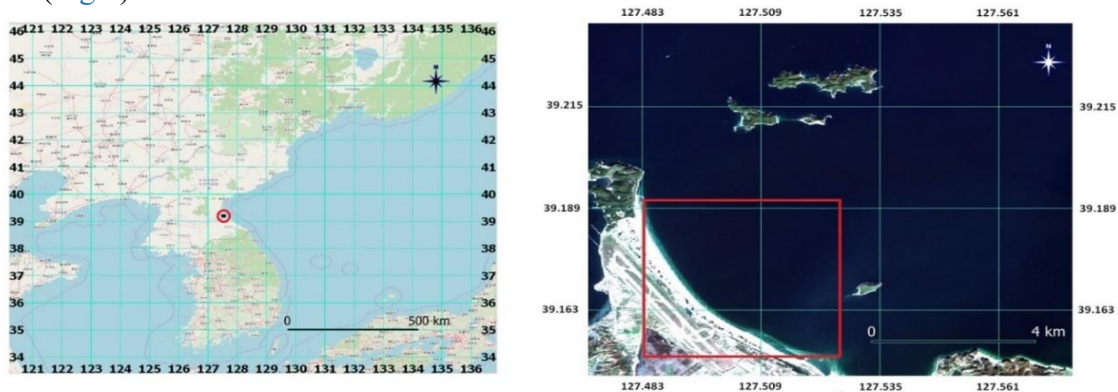

Fig.1. The location of the study area of the Wonsan Kalma Coast of the Democratic People's Republic of Korea. (a) Location of Wonsan Kalma Coast in OpenStreetMap, and (b) RGB composite of Sentinel-2A tile MSIL1C (October 30, 2019) at Wonsan Kalma Coastal research area.

The rectangle indicates the Region of Interest (ROI) for bathymetric. The length of the coastline is about 6 km, and the research area is 12.541 km².

2.2 Data Acquisition

2.2.1 Satellite Data

In this study, the Sentinel-2A Level-1C multispectral image (consisting of 13 spectral channels) obtained on October 30, 2019, was used. Level-1C data was downloaded directly from the opensource ESA / Copernicus Science Hub. The following table gives the characteristic data of the downloaded satellite image.

Table 1. Characteristics of the research area image.

Characteristic index	Result
Cloud cover percentage	0.0
Degraded ancillary data percentage	0.0
Degraded MSI data percentage	0
Format	SAFE
Format correctness	PASSED
General quality	PASSED
Geometric quality	PASSED
Pass direction	DESCENDING
Radiometric quality	PASSED
Sensor quality	PASSED

2.2.2 GEBCO data

GEBCO (General Bathymetric Chart of the Oceans) data can be downloaded directly from GEBCO 2019 Gridded Bathymetry data download (https://download.gebco.net/). The GEBCO 2019 grid, GEBCO's grid-

based survey dataset, is a global topography model for surveying oceans and lands at 15-second intervals. The GEBCO 2019 grid comes with a Type Identifier (TID) grid that provides information about the source data type. The GEBCO_2019 grid and TID grid can be downloaded as a global file in netCDF format or a set of 8 tiles ($90° \times 90°$ each) and provide a full range in Esri ASCII raster and data GeoTiff formats. The source of the GEBCO dataset is the GEBCO Compilation Group (2019) GEBCO 2019 Grid (doi: 10.5285 / 836f016a-33be-6ddc-e053-6c86abc0788e). GEBCO grid of shallow waters contains data from sources with vertical datums other than the average sea level.

3. Methodology

3.1 Selection of bathymetry model

Two models can be used to measure the water depth from a multispectral satellite image: the empirical model and the semi-analytical model. [21]

The empirical model is base on statistical models, which has established using field bathymetry data and top-of-atmosphere (ρ_{TOA}) or surface (ρ_W) reflectances derived from satellite measurements located at the same geographical location. The semi-analysis model is base on the physical model, and H can calculate as a function of ρ_W. However, the optimization of some parameters of the physical model is necessary. This procedure has usually based on a training dataset derived from field measurements. In the paper, GEBCO data that is easy to obtain is used instead of field measurement data that is difficult to obtain. The empirical model is very significant for aquatic color applications in coastal waters because it is easy to implement the algorithm and can use ρ_{TOA} directly. When calculating ρ_W, specific and complicated corrections are required to remove the atmospheric contribution to ρ_{TOA}. The disadvantage is the need to correct the statistical model for every image in the field dataset, which means that the research area should be statistically has represented. In this paper, an empirical model has selected for water depth measurement. The reason is as follows.

-the simplicity of algorithm implementation and the direct use of ρ_{TOA}

-the usefulness of GEBCO data to correct the statistical model used for bathymetry inversion

-the quasi spatial homogeneity of the optical properties over the study site

3.2 Correction of ρ_{TOA}

Satellite images (0-10 m) with high spatial resolution associated with the littoral aquatic systems generally have severe environmental noise, which must correct before any analysis. This natural noise generates the inter-pixel variability of ρ_{TOA} due to the impact of different environmental factors, which is independent of changes in depth, seawater, and substrate optical properties. One of the main factors limiting the accuracy of remotely sensed data in coastal environments is the reflection of light by the sun. Various methods have developed to modify ρ_{TOA} from sun glint. [22]

ρ_{TOA} is modified based on the following steps.

-ROI extraction related to the optically homogeneous deep waters (ROI sunglint)

-Determination of the minimum value of ρ_{TOA} (NIR) and the slope value (b) of the linear regression between ρ_{TOA} (VIS) (dependent variable) and ρ_{TOA} (NIR) (explanatory variable). NIR and VIS are associated with the spectral bands located in the near-infrared and visible wavelengths, respectively;

Correction of ρ_{TOA} (VIS) over the total ROI by applying the following formula:

$$\rho_{TOA}^{cor}(VIS) = \rho_{TOA}(VIS) + b(MIN - \rho_{TOA}(NIR)) \qquad (1)$$

Where, ρ_{TOA}^{cor} is the reflectance corrected for the sun glint in the visible spectrum, and MIN is the minimum value of $\rho_{TOA}(NIR)$.

3.3. Calibration of the bathymetry measurement model

Here, an empirical model has calibrated to obtain a bathymetry Z using a multispectral image.

The empirical model has based on the analytical formulation of Maritorena and so on [23], which establishes the relationship between the instantaneous water depth (H) and the water-leaving reflectance ρ_W :

$$H = -\frac{1}{2K}\left[\ln\left(\rho^{bottom} - \rho_W^{deep}\right) - \ln\left(\rho_W - \rho_W^{deep}\right)\right] \qquad (2)$$

Where, K (m^{-1}) is the vertically-averaged effective or operational attenuation coefficient, ρ^{bottom} is the bottom reflectance, and ρ_W^{deep} is the reflectance over optically deep waters.

For optically homogeneous areas, the values of K, ρ_W^{deep} and ρ^{bottom} can have considered as constants.

In this case, equation (2) can have simplified to obtain an empirical model given by the following formulation:

$$Z = \alpha + \beta \times \ln\left(\rho_{TOA}(G) - \rho_{TOA}^{deep}(G)\right) \qquad (3)$$

In the equation (3), G is a spectral band located in the green wavelengths, and α and β are constants that must have calculated for each image using a linear regression between GEBCO data and $\rho_{TOA}(G)$.

The choice of G-band is base on the fact that K is minimal at these wavelengths, which allows the calculation of Z for deeper depth. ρ_W has replaced by ρ_{TOA}.

This simplification is base on the fact that a linear relationship between the two parameters is assumed. Similarly, H has replaced by Z. As described above, the method for measuring the depth from a multispectral satellite image by correcting the empirical model is as follows.

-Extract GEBCO data for the research area in raster format (.TIF);

-Determination of the $\rho_{TOA}^{deep}(G)$ value using the sub-image of $\rho_{TOA}(G)$ associated with the ROIsunglint;

-From the ROI site, extraction of the ROI associated with the geographical limits of the raster image of the GEBCO data (ROIGEBCO);

-Calculation of $\ln\left(\rho_{TOA}(G) - \rho_{TOA}^{deep}(G)\right)$ for the sub-image of $\rho_{TOA}(G)$ associated with the ROIGEBCO;

-Determination of the α and β constants (equation (3)) using linear regression;

-Calculation of the bathymetry using the corrected empirical model over the whole study site;

4. Results

4.1 Extraction of the research (ROIsite) area using QGIS

The QGIS Clipper tool had used to extract the study area because the study area was smaller than the satellite image tile. In this paper, the Sentinel-2/MSI band 3 and band 8 used, because band 3 corresponds to ρ_{TOA} (VIS) and band 8 corresponds to ρ_{TOA} (NIR).

The extraction results of the research area using the QGIS Clipper tool are as follows. (Fig.3)
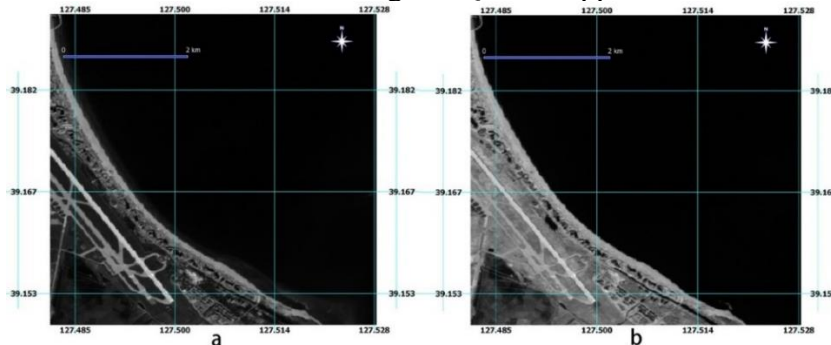

Fig.2. (a) Band 3(B03_site) and (b) band 8(B08_site) of the research area

As shown in Fig.2, the research area is composed of land and sea areas. Since the study object is the sea area, including the coast, the land area has no meaning in interpretation. If the bathymetry model

applies to the entire study area image, including the land area, it may cause negative results due to various light reflections in the land area. Therefore, the land area should remove from the study area image. To remove the land area, it prefers to analyze the histogram for the entire study area image to determine a reasonable threshold value and then to separate the land area and the sea area based on the threshold value. When analyzing the two band images in Fig.3, it can see that the band 8 spectral image is suitable for separating the land area and the sea area. The analysis results of the histogram of B08_site are as follows. (Fig.3)
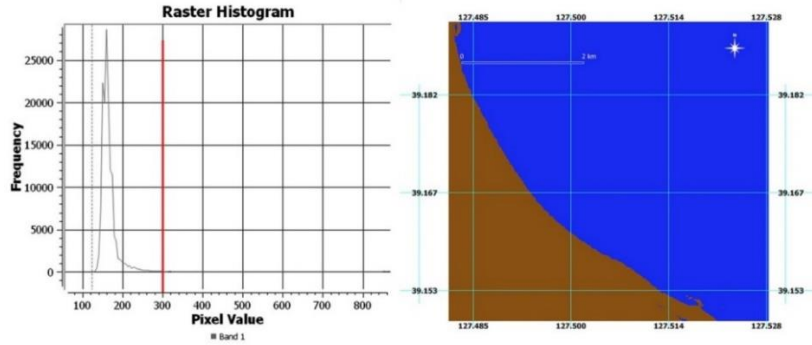
Fig.3. Histogram of band 8 spectrum image (a) and separation result of land area and sea area when the threshold value is 300 (b)

As shown in Fig.3, the best result had obtained when the threshold value was 300.

4.2 Pre-processing results for partial images

It should be divided by 1000 to convert ρ_{TOA} to reflectance value. Then, the reflectance values by the sun glint as well as them of the waves and vessels should be corrected.

To remove the influence of environmental noise, an optically uniform part is set in the research area image and extracted separately for the two bands (Fig.4).
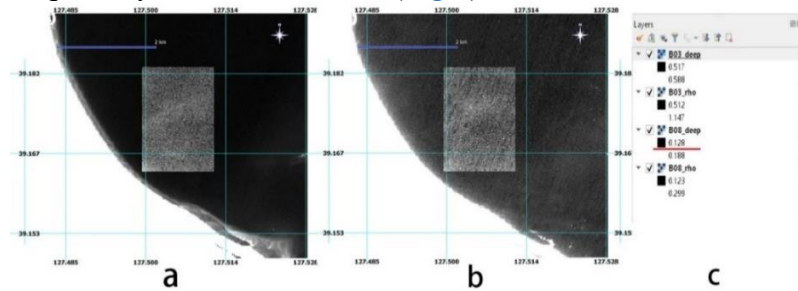

Fig.4. Data value range of band 3 spectrum image ((a) B03_rho) and band 8 spectrum image ((b) B08_rho) and partial images for correcting sun glint (B03_deep and B08_deep) (c)

In Fig.4, the value underlined in red is the minimum value of ρ_{TOA} (NIR) (MIN = 0.123).

Use r.regression.line tool of QGIS (calculate linear regression $y = a + b \times x$ from two rasters) to determine the slope value b of the linear regression between ρ_{TOA} (VIS) and ρ_{TOA} (NIR). (Table 2)

Table 2. Linear regression calculation result between B03_deep and B08_deep

Parameter	Value
a (Offset)	0.507
b (Gain)	0.240

As shown in Table 2, the value of b is 0.240. If the value of b is close to 0, it indicates that there is no correlation between ρ_{TOA} (VIS) and ρ_{TOA} (NIR). It can interpret that the environmental noise is uniform and low for the entire study area, and it can assume that the study area is optically uniform. Equation (2) can convert as follows to remove the influence of environmental noise.

$$BN\_cor = B03\_rho + b \times (MIN - B08\_rho) \qquad (4)$$

Calculate equation (4) using the Raster Calculator tool of QGIS to realize the solar glitter correction
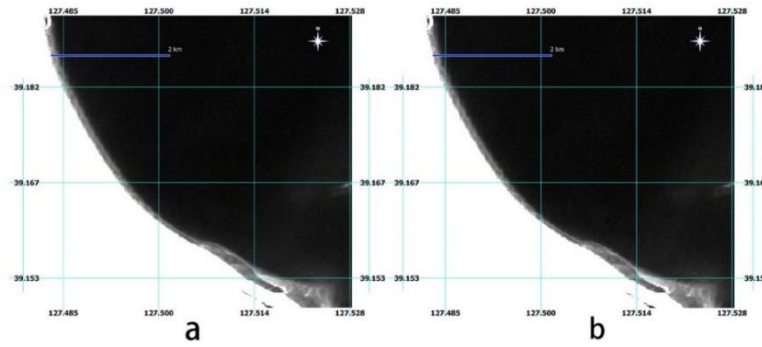
Fig.5. Environmental noise correction results ((a) pre-correction image, (b) post-correction image)

As shown in Fig. 5, it can seem that when the pre-corrected image and the post-corrected image enlarge, there is a little only difference due to the corrected result, but they are almost identical. Since the value of b is 0.240402, which is close to 0, it can regard that there is little correlation between the two images, and it is optically uniform.

4.3 Bathymetric calculation result

4.3.1 Calculation of $\rho_{TOA}^{deep}(G)$

To calculate the depth using Eq. (3), the reflectance $\rho_{TOA}^{deep}(G)$ in the deep sea must first be calculated. $\rho_{TOA}^{deep}(G)$ calculates by using the r.quantile tool of QGIS. (Fig.6)
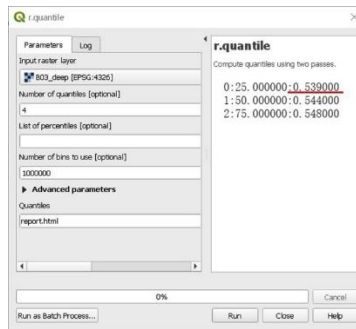

Fig.6. QGIS processing diagram used to calculate the first quartile associated with partial image B03_deep

In Fig. 6, the value indicated by the red underline is $\rho_{TOA}^{deep}(G)$. That is, $\rho_{TOA}^{deep}(G) = 0.539000$.

4.3.2 Calculation of α and β

Eq. (3) transformed again from the standpoint of spectral image analysis, is as follows.

$$Z = \alpha + \beta \times BN\_X \qquad (5)$$

To calculate $\propto$ and β for convenience, it denotes by $BN\_X = \ln(B03\_cor - 0.539)$, and the raster calculator of QGIS use to obtain the result (Fig.7).
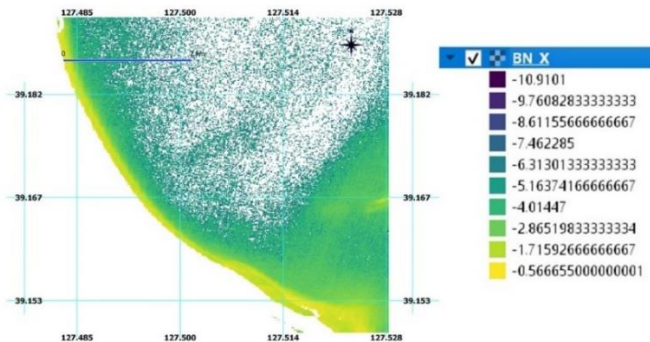

Fig.7. BN_X calculation result

α and β have obtained by performing linear regression with the BN_X and the image

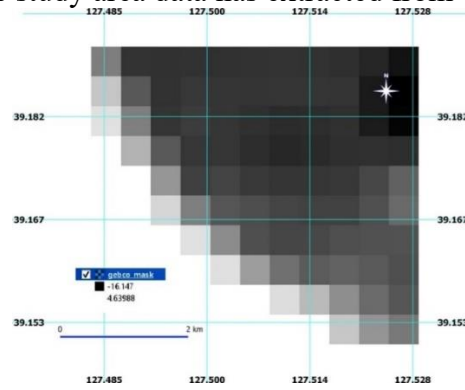(GEBCO_mask.tif) that only the study area data has extracted from GEBCO data. (Fig.8).

Fig.8. Image of extracting only research area data from GEBCO data

The result table of the linear regression conducted between BN_X and GEBCO_mask using the "r.regression.line" tool of QGIS is as follows. (Table 3)

Table 3. First-order linear regression result table between BN_X and GEBCO_mask

Parameter	Value
a (Offset)	1.718
b (Gain)	2.213

In Table 3, a corresponds to α, and b corresponds to β. From this, Eq. (6) is as follows.

$$Z = \alpha + \beta \times BN\_X = a + b \times BN\_X \qquad (6)$$

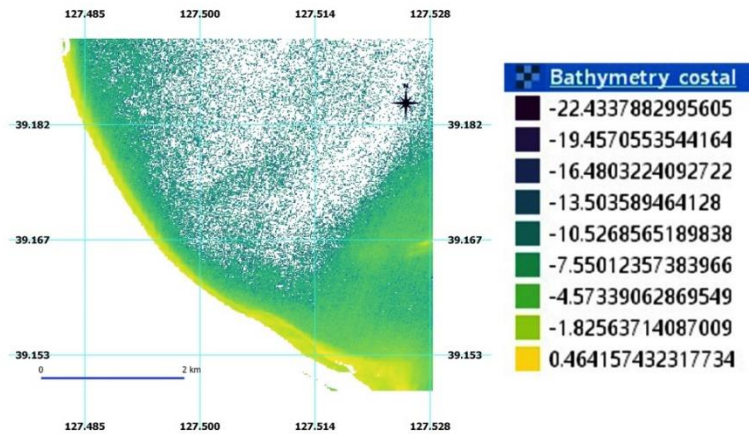The result of calculating Eq. (6) using the QGIS raster calculator is as follows (Fig.9).

Fig.9. the coastal bathymetry measurement result of the research area

As shown in Fig. 9, the depth calculation result was calculated from a wide range of -22.4m to 0.46m. In Fig. 9, the white pixels existing in the study area image have no depth value due to the calculation of the light reflectance in the deep sea and have set as no data value. It is necessary to calculate the depth value of pixels with no data value to map the depth measurement in the entire study area. Therefore, linear regression is performed between B03_cor and GEBCO_mask to obtain parameters, and B03_cor has substituted for BN_X in Eq. (6) to get the resulting image. Also, the pixels having no data values are extracted and masked, and then applied to the resulting image to obtain the depths of the pixels with no data values. The final bathymetry result for the entire research area has obtained by synthesizing the depth result of the coastal area and the depth calculation result of pixels having no data value. (Fig. 10)
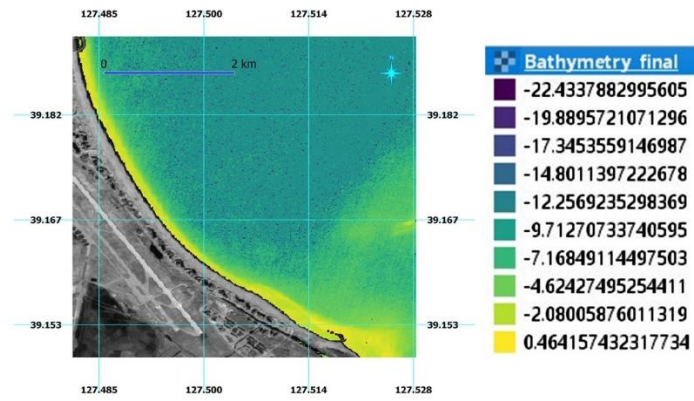
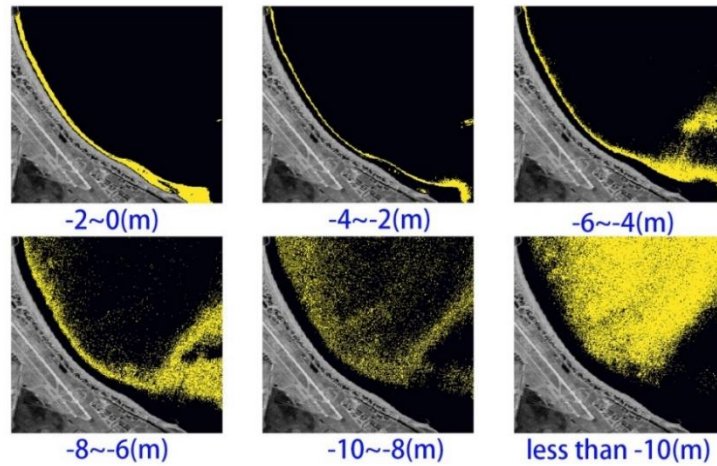Fig.10. Bathymetric calculation result for the research area

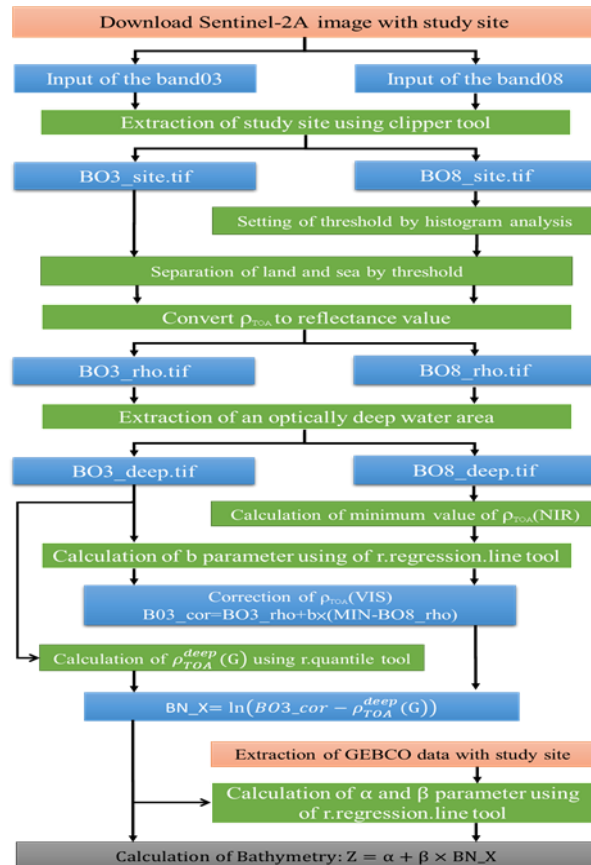Fig.11. Analysis of the results along to the bathymetric depth

5. Discussion

Fig.12. the image processing flow of QGIS

In this study, a methodology for measuring the coast depth has established by combining the Sentinel-2A satellite image, which is a multi-spectral satellite image, and a bathymetric dataset of GEBCO. Then it has applied to the study area, so to Fig. the bathymetric measurement map for the research object. As a result of analyzing previous studies for establishing a bathymetry model, an empirical model based on a statistical model has selected. Eq. (6) has established using the relationship between the parameters of the empirical model and the bands of the Sentinel-2A image. Besides, research has conducted to remove the sun glittering, which is a major factor restraining the accuracy of remotely received data in the marine environment, and Eq. (4) applied to the research object to obtain a new result. That is, the closer the value of b is to 0 in Eq. (4), the more optically uniform it is, and the higher accuracy can ensure in-depth calculation. The entire process of implementing the proposed method could realize smoothly by using the powerful spatial analysis tools of QGIS. The image processing flow of QGIS for the proposed method give below. (Fig. 12)

6. Conclusions

Radar bathymetric depths on ships that primarily used in coastal measurements are sometimes unavailable or very expensive. And due to the coastal dynamics, precision is wrong, and often repeated measuring problems happen. This study could calculate bathymetric depth in a broad coastal area using Sentinel-2A satellite images and GEBCO data, which can be downloaded for free from the website at any time. Therefore, without field bathymetry data, it is easy to measure a wide range of coastal water depths in a short time using this method. Based on the scientific analysis of the correspondence between the spectral band images of Sentinel-2A and the factors of the experiential model, it has converted into a practical depth measurement model. As a result of applying the proposed depth measurement model in the study area to the study area, 95% prediction accuracy guaranteed over a wide range of -22.4m to 0.46m. To increase measurement accuracy, suitable atmospheric conditions and an optically uniform satellite image should select, and the water level caused by the tide should consider. This research can not only compile a water depth survey map of the coast but also visually display the morphological evolution of sediments under the water.

Therefore, from environmental monitoring to the formulation of seabed maps and coastal management, it is applicable to many important fields.

REFERENCES

[1] Liang B , Wu G , Liu F , et al. Numerical study of wave transmission over double submerged breakwaters using non-hydrostatic wave model[J]. Oceanologia, 2015:S0078323415000913.

[2] Liang B, Shao Z, Wu G, et al. New equations of wave energy assessment accounting for the water depth [J]. Applied Energy, 2017, 188(Complete):130-139.

[3] Shao Z, Liang B, Li H, et al. Blended wind fields for wave modeling of tropical cyclones in the South China Sea and East China Sea [J]. Applied Ocean Research, 2018, 71:20-33.

[4] Liang B, Shao Z, Li H, et al. An automated threshold selection method based on the characteristic of extrapolated significant wave heights [J]. Coastal engineering, 2019, 144(FEB.): 22-32.

[5] Liu, Guijie, and et al. "A mini review of recent progress on vortex-induced vibrations of marine risers." Ocean Engineering (2019): 106704.

[6] Yan, Zhiduo, et al. "Ultra-long return level estimation of extreme wind speed based on the deductive method." Ocean Engineering 197 (2020): 106900.

[7] Wu G, Shi F, Kirby J T, et al. Modeling wave effects on storm surge and coastal inundation [J]. Coastal Engineering, 2018, 140(OCT.):371-382.

[8] Cheng L, Ma L, Cai W, et al. Integration of Hyperspectral Imagery and Sparse Sonar Data

for Shallow Water Bathymetry Mapping [J]. IEEE Transactions on Geoscience & Remote Sensing, 2015, 53(6):3235-3249.

[9] E.W.J.Bergsma, D.C.ConleyM.A.Davidson, T.J.O'Hare. Video-based nearshore bathymetry estimation in macro-tidal environments [J]. Marine Geology, 374:31-41.

[10] Hodúl, Matúš, et al. "Satellite derived photogrammetric bathymetry." ISPRS Journal of Photogrammetry and Remote Sensing 142 (2018): 268-277.

[11] Rutten J, Jong S M D, Ruessink G. Accuracy of Nearshore Bathymetry Inverted From X-Band Radar and Optical Video Data [J]. IEEE Transactions on Geoscience & Remote Sensing, 2016, PP (99):1-11.

[12] Lu T , Chen S , Tu Y , et al. Comparative Study on Coastal Depth Inversion Based on Multi-source Remote Sensing Data[J]. Chinese Geographical Science, 2019, 29(2):192-201.

[13] Vyas, N. K., and H. I. Andharia. "Coastal bathymetric studies from space imagery." Marine Geodesy 12.3 (1988): 177-187.

[14] Patricio A. Catálan, Haller M C. Remote sensing of breaking wave phase speeds with application to non-linear depth inversions [J]. Coastal Engineering, 2008, 55(1):93-111.

[15] Holland K T , Lalejini D M , Spansel S D , et al. Littoral Environmental Reconnaissance Using Tactical Imagery From Unmanned Aircraft Systems[J]. Proceedings of Spie the International Society for Optical Engineering, 2010, 7678(5):767806-767806-8.

[16] Yoo J , Fritz H M , Haas K A , et al. Depth Inversion in the Surf Zone with Inclusion of Wave Nonlinearity Using Video-Derived Celerity[J]. Journal of Waterway Port Coastal & Ocean Engineering, 2011, 137(2):p.95-106.

[17] Holman R A, Holland K T, Lalejini D M, et al. Surf zone characterization from Unmanned Aerial Vehicle imagery [J]. Ocean Dynamics, 2011, 61(11):p.1927-1935.

[18] Holman R, Plant N, Holland T. CBathy: A robust algorithm for estimating nearshore bathymetry [J]. Journal of Geophysical Research Oceans, 2013, 118(5).

[19] Sun S H, Chuang W L, Chang K A, et al. Imaging-Based Nearshore Bathymetry Measurement Using an Unmanned Aircraft System [J]. Journal of Waterway Port Coastal & Ocean Engineering, 2019, 145(2).

[20] Tissier M, Bonneton P, Almar R, et al. Field measurements and non-linear prediction of wave celerity in the surf zone [J]. European Journal of Mechanics, B/Fluids, 2011, 30(6):635-641.

[21] Capo, Sylvain, et al. "Assessment of the decadal morphodynamic evolution of a mixed energy inlet using ocean color remote sensing." Ocean Dynamics 64.10 (2014): 1517-1530.

[22] Bru D. Corrections atmosphériques pour capteurs à très haute résolution spatiale en zone littorale [J]. 2016.

[23] Stéphane, Maritorena, and André, et al. Diffuse reflectance of oceanic shallow waters: Influence of water depth and bottom albedo [J]. Limnology & Oceanography, 1994.